Published in final edited form as:
Dev Biol. 2007 June 1; 306(1): 193–207. doi:10.1016/j.ydbio.2007.03.013.

The MAPK$^{ERK-1,2}$ pathway integrates distinct and antagonistic signals from TGFα and FGF7 in morphogenesis of mouse mammary epithelium

Jimmie E. Fata[a,*], **Hidetoshi Mori**[a], **Andrew J. Ewald**[b], **Hui Zhang**[a], **Evelyn Yao**[a], **Zena Werb**[b], and **Mina J. Bissell**[a,*]

[a]Life Sciences Division, Lawrence Berkeley National Laboratory, Berkeley, CA 94720, USA

[b]Department of Anatomy, University of California, San Francisco, CA 94143, USA

Abstract

Transforming growth factor-α (TGFα) and fibroblast growth factor-7 (FGF7) exhibit distinct expression patterns in the mammary gland. Both factors signal through mitogen-activated kinase/extracellular regulated kinase-1,2 (MAPK^{ERK1,2}); however, their unique and/or combined contributions to mammary morphogenesis have not been examined. In ex vivo mammary explants, we show that a sustained activation of MAPK^{ERK1,2} for 1 h, induced by TGFα, was necessary and sufficient to initiate branching morphogenesis, whereas a transient activation (15 min) of MAPK^{ERK1,2}, induced by FGF7, led to growth without branching. Unlike TGFα, FGF7 promoted sustained proliferation as well as ectopic localization of, and increase in, keratin-6 expressing cells. The response of the explants to FGF10 was similar to that to FGF7. Simultaneous stimulation by FGF7 and TGFα indicated that the FGF7-induced MAPK^{ERK1,2} signaling and associated phenotypes were dominant: FGF7 may prevent branching by suppression of two necessary TGFα-induced morphogenetic effectors, matrix metalloproteinase-3 (MMP-3/stromelysin-1), and fibronectin. Our findings indicate that expression of morphogenetic effectors, proliferation, and cell-type decisions during mammary organoid morphogenesis are intimately dependent on the duration of activation of MAPK^{ERK1,2} activation.

Keywords

MAPK^{ERK1,2}; Kinetics; Mammary; Branching; Morphogenesis; TGFα; FGF7

Introduction

Branch formation in the mammary gland results from an intricate interplay between cell intrinsic and extrinsic factors. These extracellular factors can be grouped broadly into, but not limited to, hormones, growth factors, proteases, and the extracellular matrix (ECM), each of which have been demonstrated to be required for normal mammary development (Fata et al., 2004; Hovey et al., 2002; Parmar and Cunha, 2004; Schedin et al., 2004; Sternlicht, 2006).

*Corresponding authors. 1 Cyclotron Rd, Berkeley, CA 94710 MS977R225A, USA. Fax: +1 510 486 5586. jefata@lbl.gov (J.E. Fata), mjbissell@lbl.gov (M.J. Bissell).

Appendix A. Supplementary data

Supplementary data associated with this article can be found, in the online version, at doi:10.1016/j.ydbio.2007.03.013.

Members of the epidermal and fibroblast growth factor receptor (EGFR, FGFR) families are required for normal mammary development (Mailleux et al., 2002; Sternlicht, 2006), and a number of growth factors have been shown to have functional roles including EGFR and FGFR ligands (Luetteke et al., 1999; Mailleux et al., 2002; Sternlicht et al., 2005). A major unresolved question is how these signals are temporally integrated to generate the diverse range of morphogenetic behaviours observed during mammary development and differentiation.

The mitogen-activated protein kinase (MAPK) pathway includes a three kinase cassette of Rous sarcoma associated factor (Raf), mitogen-activated protein/ERK kinase (MEK), and extracellular regulated kinase (ERK), producing a sequential activation pathway responsive to a diverse array of extracellular stimuli (Roux and Blenis, 2004). A fundamental question of signal transduction is how the canonical components of the MAPK pathway, Raf→MEK → ERK, integrate signals from multiple stimuli into distinct cellular outcomes (Marshall, 1995; Schlessinger, 2004). For instance, the rat pheochromocytoma PC12 cell line proliferates in response to EGF but differentiates in response to nerve growth factor (NGF), although both stimuli elicit activation of the Raf → MEK → ERK cassette (Qui and Green, 1992; Traverse et al., 1992). Efforts into resolving this question have focused on the duration of the signal through ERK-1 and ERK-2 ($MAPK^{ERK1,2}$) as a key factor determining the fate of a single cell or groups of cells grown on tissue culture plastic. Intense $MAPK^{ERK1,2}$ phosphorylation is evident by whole-mount immunohistochemistry in the course of the development of certain organs during mouse embryogenesis, including the branchial arches, limbs, and lung buds (Corson et al., 2003). Prolonged activation of $MAPK^{ERK1,2}$, in response to hepatocyte growth factor, is associated with immortalized kidney cells undergoing tubulogenesis in collagen type-1 gels (Karihaloo et al., 2004; Maroun et al., 1999). Signalling through the $MAPK^{ERK1,2}$ pathway is necessary for the development of branched organs such as the lung (Kling et al., 2002), kidney (Hida et al., 2002), and salivary gland (Kashimata et al., 2000), but whether the duration of $MAPK^{ERK1,2}$ phosphorylation is indeed a developmentally relevant regulator of organogenesis has not been addressed.

To examine the interplay between growth factor signals, $MAPK^{ERK1,2}$ activation, and mammary branching morphogenesis, we utilized an organotypic 3D mammary primary culture that models aspects of branching morphogenesis in vivo and is responsive to growth factors produced in the mammary gland. In this assay, the mammary epithelium is separated from most of the stroma but retains epithelial/myoepithelial spatial organization, allowing us a framework to evaluate the precise role of signalling modules in a controlled and reproducible environment. We show that individually as well as in combination, TGFα and FGF7 elicit distinct kinetics of $MAPK^{ERK1,2}$ activation that in turn predicts both cellular and morphogenetic outcomes.

Materials and methods

Isolation of primary mammary organoids

The 4th inguinal mammary glands were removed from 10 to 14 weeks old virgin Balb/c mice and minced with two parallel razor blades (approved by the Animal Welfare and Research Committee (AWRC) at Lawrence Berkeley Labs; animal protocol #0522). At this age the expansion of the ductal tree within the fat pad is complete and no terminal end buds exist. Minced tissue (4–8 glands) was gently shaken for 30 min at 37 °C in a 50-ml collagenase/trypsin mixture (0.2% trypsin, 0.2% collagenase type IV, 5% fetal calf serum, 5 μg/ml Insulin, 50 μg/ml gentamycin, in 50 ml of DMEM/F12). The collagenase solution was discarded after centrifugation at 1000 rpm and the pellet was re-suspended in 10 ml DMEM/F12. The suspension was pelleted again at 1000 rpm for 10 min, re-suspended in 4 ml of DMEM/F12 +40 μl of DNase (2 U/μl), and incubated for 5 min at ambient temperature with occasional shaking. The DNase solution was removed after centrifugation at 1000 rpm for 10 min. The

DNase solution was discarded and the epithelial pieces were separated from the single cells through differential centrifugation. The pellet was re-suspended in 10 ml of DMEM/F12 and pulsed to 1500 rpm. The supernatant was then removed and the pellet was re-suspended in 10 ml DMEM/F12. Differential centrifugation was performed at least 4 times. The final pellet was re-suspended in the desired amount of medium or Matrigel (Growth Factor Reduced Matrigel, BD Biosciences, San Jose, CA).

Morphogenesis assay

Morphogenesis assays were performed in 96 well culture plates. The culture had two layers, an underlay of 50 μl of Matrigel (Growth Factor Reduced Matrigel, BD Biosciences) and an overlying layer of organoids suspended in Matrigel. The underlay was allowed to set for 30 min at 37 °C, and then a 50-μl suspension of organoids in Matrigel (~100–200 organoids/100 μl of Matrigel) was added to the well followed by an incubation of 30 min at 37 °C. All wells were then treated with 150 μl of basal media (DMEF/F12 with 1% insulin, transferrin, selenium, and 1% penicillin/streptomycin) for 24 h. After 24 h the basal media was replenished (untreated samples) or growth factors TGFα (9 nM; Sigma, Saint Louis, MO), FGF7 (9 nM; Sigma, Saint Louis, MO), or FGF10 (9 nM; Biosource, Camarillo, CA) were added to basal media individually or in combinations. Every other day all samples were replenished with basal media alone. To determine the morphogenic response we counted all organoids within each well (~100–200 organoids/well) having 3 or more branches and divided this number by the total number of organoids per well (Simian et al., 2001). For inhibition of $MAPK^{ERK1,2}$ signaling, PD98059 (Calbiochem, San Diego, CA) was added to growth factor-supplemented medium at a concentration of 40 μM. Inhibition of MMP-3 was accomplished with 30 μM of an MMP-3-specific peptide-based inhibitor containing the sequence Ac-Arg-Cys-Gly-Val-Pro-Asp-NH_2 (Calbiochem). The broad based metalloproteinase inhibitor, GM6001, was added to media at 40 μM. Inhibition of fibronectin adhesion was accomplished with blocking antibodies against α5β1-integrin (Chemicon, Temecula, CA) at a concentration of 2 μg/ml.

RT-PCR

Total RNA was isolated with QIAGEN RNeasy Mini Kit (Valencia, CA). For cDNA synthesis, 20 ng of total cellular RNA was used to synthesize cDNA using SuperScript III First-Strand Synthesis System (Invitrogen, Carlsbad, CA). MMP-3 was amplified with GTTCCTGATGTTGGTGGCTT and AGCCTTGGCTGAGTGGTAGA primers. Primers that detect fibronectin were TACCAAGGTCAATCCACACCCC and CAGATGGCAAAAGAAAGCAGAGG. As a control for total RNA, RT-PCR for GAPDH was performed with primers TGAAGGTCGGTGTGAACGGATTTGGC and CATGTAGGCCATGAGGTCCACCAC. The amplified fragments were resolved on 1% agarose gels and products were detected with a FluorChem 8900 analysis system (Alpha Innotech, San Leandro, CA). Real-time PCR was performed using LightCycler System (Roche Diagnostics, Indianapolis, IN) according to the manufacturer's instructions. Fast Start DNA Master SYBR Green I (Roche Diagnostics, Indianapolis, IN) was used for PCR reaction. PCR data were analyzed with LightCycler Software ver.3 (Roche Diagnostics, Indianapolis, IN). Relative signals between fibronectin or MMP3 and 18s rRNA were quantified.

Protein isolation

For protein isolation, media were removed from the well, and Matrigel + organoids were washed once with cold 1× PBS containing NaF (1 mM) and Na_3VO_4 (1.25 mM). Matrigel and organoids were then treated with a 3D lysis solution consisting of 90% NP40 lysis mix (50 mM Tris–HCl, pH 8.0, 5 mM EDTA, 150 mM NaCl, 0.5% NP40) plus 10% 10× SDS loading buffer (83.3 μl 12 M acetate [70% glacial acetic acid (17.4 M) and 30% water], 3.67 ml water, 1.25 μl 2-mercaptoethanol, 0.01 g bromophenol blue, 5.0 ml glycerol, 1 g SDS). Samples were

pipetted up and down and stored at −20 °C. The 3D lysis solution was heated to 65 °C just prior to using.

Immuno-detection of MAPK^{ERK1,2} phosphorylation

For immunoblot analysis, protein samples were heated at 65 °C for 5 min then placed on ice for 3–5 min. Samples were centrifuged at 13000 rpm for 5 min and the soluble portion was resolved on a pre-cast 10% Tris–glycine polyacrylamide gel (InVitrogen, Carlsbad, CA) using the NOVEX system (InVitrogen, Carlsbad, CA). Resolved proteins were transferred to Hybond nitrocellulose (Amersham, Piscataway, NJ) followed by blocking in 1× TBS, 0.1% Tween-20 with 5% w/v non-fat dry milk for 1 h at ambient temperature. Membranes were incubated overnight at 4 °C in 5% BSA, 1× TBS, 0.1% Tween-20 containing rabbit anti-human polyclonal antibodies that recognize either phosphorylated MAPK^{ERK1,2} (Thr202/Tyr204, #9101, Cell Signaling Tech., Beverly, MA), phosphorylated MEK1 (Ser 298, #9128, Cell Signaling Tech., Beverly, MA), total MAPK^{ERK1,2} (–9102, Cell Signaling Tech., Beverly, MA), or beta-Actin (–4967, Cell Signaling Tech., Beverly, MA). In some cases, determination of total MAPK was performed on separate membranes using identical samples. Primary antibodies were detected with the Pierce SuperSignal detection kit (Rockford, IL) and signal was captured with the FluorChem 8900 analysis system (Alpha Innotech, San Leandro, CA).

Immunocytochemical detection of Ki67, keratins, and receptors

For detection of Ki67, keratin-8 (K8), keratin-14 (K14), and keratin-6 (K6), a mixture of 18% sucrose in PBS (15 min at ambient temperature) followed by 30% sucrose (15 min at ambient temperature) was applied to organoids in Matrigel to maintain organoid structure. After sucrose treatment, organoids in Matrigel were gently pipetted up and down and then smeared onto a glass slide. Smeared organoids were allowed to dry at ambient temperature for 2 h and then fixed in methanol: acetone (1:1 v/v) at −20 °C for 10 min. After fixation, slides were air-dried at ambient temperature for 2 h followed by blocking in 10% sheep serum in PBS for 1 h at ambient temperature. The primary antibodies, rabbit polyclonal anti-human Ki67 (Ki67p, Novocastra, UK), rat monoclonal anti-mouse K8 (Troma-1, Iowa DSHB, Iowa City), mouse monoclonal anti-human K14 (clone #LL002, Novocastra, UK), rabbit polyclonal anti-mouse-K6 (PRB-169P, Covance Research Products, Berkeley), goat polyclonal anti-human FGFR2 (Bek N-20, Santa Cruz Biotechnology, Santa Cruz, CA), and rabbit polyclonal anti-human EGFR (–2232, Cell Signaling Tech., Beverly, MA) were incubated in blocking buffer overnight at 4 °C, followed by 3 × 15 min washes in 0.5% Triton-X in PBS. For detection of primary antibodies, appropriate fluorophore-labeled secondary antibodies were used and images were captured using confocal microscopy. The generation of confocal stack montages and generation of threshold images for calculating double positive keratin cells were accomplished with ImageJ (NIH).

Live–dead cell detection

To determine the ratio of live to dead cells, we used Molecular Probes (Carlsbad, CA) LIVE/DEAD Viability/Cytotoxicity Kit, which provides a two-color discrimination of live and dead cell populations. For live cells a membrane permeant calcein AM, which is cleaved by intracellular esterases in live cells to yield cytoplasmic green fluorescence, was added to the assay. Dead cells, which have a compromised plasma membrane, were stained with the membrane impermeant nucleic acid dye, ethidium homodimer-1 yielding a red fluorescence. Both labels were incubated for 30 min at 37 °C and then visualized by fluorescent microscopy after excitation.

Real-time microscopy

Time-lapse movies were collected on a Zeiss Axiovert S-100 microscope using a 10× A-Plan objective lens and a Cohu high performance CCD camera. The light exposure was regulated by a Ludl shutter and controller, which also controlled the Ludl *x–y–z* motorized stage. Temperature was held at 37 °C and carbon dioxide at 5% using a CTI Controller 3700 and Temperature Control 37.2 combination. Images were acquired at each of 48 positions every 15 min using a custom macro implemented in OpenLab 4.0.2. (Improvision Inc., Lexington, Mass).

Results

TGFα induces branching morphogenesis in primary mammary organoids cultured within a 3D ECM gel

To examine mammary morphogenesis, we developed an organotypic 3D culture system consisting of primary mammary organoids (which contain both the epithelium and the myoepithelium, but not the adipogenic stroma) within a 3D laminin-rich extracellular matrix (3D lrECM; Matrigel). The basal medium is chemically defined (see Materials and methods) and was designed to support cell survival, but not induce branching morphogenesis (Fig. 1A). TGFα in concentrations between 1 nM and 100 nM were added to the organoids, and all doses were sufficient to induce branching. We chose a dose of 9 nM for TGFα for all experiments described because it was shown previously by us that 9 nM of EGF induces branching morphogenesis of mammary organoids in collagen type I gels (Simian et al., 2001). Branching occurred with similar frequency and pattern whether we added TGFα to the medium only once in the beginning of the assay or every other day (data not shown). Time-lapse microscopy showed that branch formation in TGFα-treated organoids was evident within the first 48 h, with the majority of bud initiation and extension observed between 48 and 72 h (Fig. 1A and Supplemental Movie 1). Branch extension, however, was limited, often resulting in a short stalk. Untreated organoids did not initiate new branches but reorganized to form acinar-like structures (Fig. 1A and Supplemental Movie 2).

FGF7 suppresses TGFα-induced morphogenesis

The mammary gland undergoes a diverse range of morphogenetic transformations during puberty, pregnancy, lactation, and involution. Which growth factors act in what combination to bring about this diversity is still poorly understood. We chose to examine the known mammary mitogens, TGFα and FGF7, since the two factors exhibit both distinct and overlapping temporal and spatial regulation. TGFα is expressed primarily in mammary epithelial cells and is elevated during branching morphogenesis and pregnancy-induced alveologenesis (Liscia et al., 1990). FGF7 is expressed primarily in the stroma, is high prior to the onset of extensive branching and declines thereafter, becoming minimal during alveologenesis (Mailleux et al., 2002; Pedchenko and Imagawa, 2000). We asked whether the actions of these two factors through $MAPK^{ERK1,2}$ were in fact redundant for morphogenesis or whether the response of organoids to FGF7 was distinct from that of TGFα. Whereas TGFα induced branching, FGF7 induced growth (Fig. 1B and Supplemental Movie 3). Morphometric analysis showed that approximately 80% of organoids produced branches within 5 days in response to TGFα; the rest resembled the untreated controls (Fig. 1C). Surprisingly, when FGF7 was added together with TGFα, it suppressed TGFα-induced branching in a dose-dependent fashion (Figs. 1B and C). A ratio of 4:1 (FGF7:TGFα) led to an approximately 80% inhibition of morphogenesis in comparison to TGFα alone (Fig. 1C). Time-lapse video microscopy indicated that unlike TGFα alone, FGF7 + TGFα induced extensive lumen expansion, and those organoids that did branch were aberrant with morphologies similar to FGF7 alone (Figs. 1B and C and Supplemental Movie 4), indicating that the FGF7 phenotype was dominant over TGFα-induced branching.

TGFα and FGF7 induce distinct MAPK^{ERK1,2} phosphorylation kinetics

TGFα and FGF7 signal through different receptors, yet each ligand is a potent activator of MAPK^{ERK1,2}. To understand how TGFα and FGF7 lead to such dramatically different morphogenetic outcomes despite using the same signalling pathway, we assayed the phosphorylation kinetics of MEK1 and MAPK^{ERK1,2} by immunoblotting protein lysates that were isolated at discrete time points after growth factor stimulation using anti-phospho-MEK/MAPK^{ERK1,2} antibodies. TGFα stimulation induced rapid phosphorylation of both MEK1 (Fig. 2A) and MAPK^{ERK1,2} (Fig. 2B), which peaked as early as 15 min and was sustained for up to 1 h. Between 1 and 2 h after TGFα stimulation, phospho-MEK1 and phospho-MAPK^{ERK1,2} levels decreased but remained well above the basal levels for at least 24 h (Figs. 2A, B and data not shown). FGF7 stimulation of organoids also led to induction of both MEK1 and MAPK^{ERK1,2} phosphorylation, but in contrast to TGFα, high levels of these kinases were evident for only 15 min (Figs. 2A, B).

Since we already knew that simultaneous addition of FGF7 and TGFα leads to a morphogenetic outcome similar to that of FGF7 alone, it was not surprising that the phospho-MAPK^{ERK1,2} duration also resembled the FGF7-like pattern (Fig. 2B). Quantification of the kinetics of phospho-MAPK^{ERK1,2} levels revealed a significant difference in the first 3 h between organoids stimulated with TGFα compared to organoids stimulated with FGF7 alone or with both FGF7 and TGFα (Fig. 2C; $*p<0.05$).

A brief window of TGFα-induced MAPK^{ERK1,2} activation sustains a prolonged morphogenetic program

Given the results obtained above, we asked (a) whether the MAPK pathway was responsible for the morphogenetic outcome and (b) whether the initial signal activated by TGFα could be sufficient to elicit the entire 5-day morphogenetic program. Pre-treatment of organoids with PD98059 (20 μM), an inhibitor of MAPK^{ERK1,2} phosphorylation for 1 h prior to TGFα stimulation inhibited MAPK^{ERK1,2} activation (Fig. 3A), and abolished branching morphogenesis (Fig. 3Bb and Supplemental Movie 5; compare to TGFα treatment alone (Fig. 3Ba) and Supplemental Movie 1). Similar results were seen when PD98059 (40 μM) was added simultaneously with TGFα (Fig. 3Bc). However, addition of PD98059 at 1, 4, 24, 48, or 72 h, post-TGFα stimulation, yielded a partial decrease in branching morphogenesis (Fig. 3Bb; and data not shown), indicating that the initial 1 h phosphorylation of MAPK^{ERK1,2} was necessary and sufficient for transducing the MAPK^{ERK1,2}-dependent component of the TGFα signal for branching. PD98059 added 1 h after TGFα stimulation was effective in inhibiting branches in 50% of organoids vs. 10% when it was added 4 h after TGFα stimulation (Fig. 3Be; compare to TGFα stimulation alone). The incomplete response to 1 h of TGFα activation suggests that additional and as yet undetermined factors may be necessary to allow the organoids to fully respond to TGFα. However, the inability of PD98059 to significantly inhibit branching after 4 h indicate that the majority of molecules necessary for branching are induced before the 4-h period. It should also be noted that it is not possible to tightly control ERK activation kinetics with PD98059 since the inhibitor functions by inactivating MEK that is not activated and does not affect activated MEK (Ballif and Blenis, 2001).

MMP-3 and fibronectin mediate TGFα-induced mammary morphogenesis

To investigate MAPK^{ERK1,2}-dependent downstream effectors of TGFα-induced morphogenesis, we screened candidate genes suspected of being involved in branching using quantitative RT-PCR on samples isolated after TGFα stimulation with or without PD98059. In a screen of a panel of a number of factors reported to be necessary for branching which included matrix metalloproteinase-3 (MMP-3), MMP-9, MMP-14, tissue inhibitor of metalloproteinase-1 (Timp-1), urokinase plasminogen activator (uPA), epimorphin (EPM), and Twist, only MMP-3 and fibronectin registered positive as being both induced by TGFα

and dependent on $MAPK^{ERK1,2}$ activation (Fig. 4A, and data not shown). In the absence of TGFα, MMP-3 and fibronectin mRNA expression was relatively low (Fig. 4A; the level of MMP-3/18s was 0.23±0.2 and that of fibronectin/18s was 0.25±0.4—data are presented as mean ratio of each mRNA/18s rRNA±standard deviation as determined by quantitative real-time PCR). After TGFα stimulation, MMP3 and fibronectin mRNA displayed a 9-fold induction (Fig. 4A; MMP-3/18s, 2.18±0.2; fibonectin/18s, 3.37±0.9). Up-regulation of both MMP-3 and fibronectin by TGFα was suppressed significantly when PD98059 was added to the cultures (Fig. 4A; 0.70±0.30 MMP-3/18s and 0.86±0.3 fibronectin/18s). Importantly, FGF7 added alone failed to induce MMP-3 and fibronectin (data not shown), and when added with TGFα, it significantly suppressed the TGFα-induced up-regulation of fibronectin (0.56±0.03 vs. 2.18±0.2 fibronectin/18s; Fig. 4B). Interestingly, TGFα-induced MMP-3 up-regulation was inhibited by only 50% (1.48±0.89 vs. 3.37±0.9 MMP-3/18s; p=0.08) in the presence of FGF7.

To test whether these candidate genes were necessary for TGFα-induced morphogenesis, we inhibited MMP-3 by a relatively selective peptide-based inhibitor (MMP-3 Inhibitor I). Morphogenesis was suppressed by about ~50%, often resulting in cyst-like structures containing a few stunted branches (Fig. 4C). However, a broad-spectrum inhibitor against all MMPs (GM6001) completely abolished branching and led to either small, underdeveloped acini (similar to Fig. 3Bb) or large, cyst-like structures as seen also with MMP-3 Inhibitor 1 (Fig. 4C).

Fibronectin inhibition was achieved by preventing its binding to its major receptor, α5β1 integrin, using inhibitory antibodies. Morphogenesis was completely suppressed in approximately 40% of the organoids compared to the control antibodies which did not suppress (Fig. 4D). Those structures that did form in the presence of the inhibitory antibody had abnormal and often thick, underdeveloped branches (Fig. 4D). Thus, while other factors may be required, it is clear that both these candidate genes are necessary for TGFα induction of branching.

$MAPK^{ERK1,2}$ regulates organoid proliferation and apoptosis

It has been argued that differentiation and growth are often incompatible in morphogenesis. To additionally explore the underlying reasons for the differences in response, we explored whether TGFα and FGF7 elicited different growth responses from the organoids. At day 2, organoids treated with TGFα, FGF7, or a combination of the two, had significantly higher Ki67-positive cells than untreated organoids (Figs. 5A, C). The TGFα-induced proliferation was dependent on $MAPK^{ERK1,2}$ activation since it was completely suppressed in organoids pre-treated with PD98059 (Figs. 5A, C). By day 4, TGFα-treated organoids stopped growing as shown by the absence of Ki67-positive cells (Fig. 5A) whereas organoids treated with FGF7 or FGF7 plus TGFα continued to proliferate, albeit to a lesser extent than seen on day 2 (Figs. 5A, C). Thus, the difference in mode of action of the two growth factors is not due to differences in the initial growth phase but may result partially from continued proliferation in the presence of FGF7.

To complete the analysis, we measured cell death under these different conditions. A significant number of dead cells were evident at both day 2 and day 4 in untreated organoids or in TGFα-stimulated organoids when pre-treated with PD98059 (Figs. 5B, C). In contrast, none of the growth factor-treated organoids had appreciable dead cells either at days 2 or 4, and there were no significant differences between TGFα- and FGF7-treated organoids (Figs. 5B, C). Thus, the kinetics of proliferation, and not apoptosis, is an additional defining feature associated with the different morphogenetic response of the two growth factors.

TGFα and FGF7 retain myoepithelial–epithelial polarity

We have shown that acinar polarity is crucial in determining the rate of apoptosis in response to a number of chemother-apeutic agents and also a significant feature distinguishing normal and malignant epithelial cells (Weaver et al., 2002). The absence of a difference in apoptosis raised the possibility that the juxtaposition of the myoepithelial/epithelial cells, which determines basal tissue polarity (Gudjonsson et al., 2002), may be different under the two conditions. We performed immunocytochemistry using antibodies against K14 and K8, which detect myoepithelial and luminal epithelial cells, respectively. Confocal microscopic analysis of K14 immunostaining after 1 day of culture revealed that untreated organoids maintained a basal layer of K14-positive myoepithelial cells possessing long cellular processes and an inner layer of K8-positive luminal epithelial cells (Fig. 6A). Myoepithelial cells were numerous and they did not completely encapsulate the organoids but instead appeared to be woven around the luminal epithelial cells (Fig. 6A). Thus, the luminal epithelium is likely to have extensive direct contact with the BM, an arrangement that is observed also in vivo (Emerman and Vogl, 1986).

Organoids that had undergone branching morphogenesis after TGFα treatment had a similar spatial arrangement; with K14 myoepithelial cells surrounding K8 epithelial cells (Fig 6B). Intriguingly, a large subset (17.5±3%) of the cells co-expressed both K14 and K8 (yellow in merged images Fig. 6B; Supplemental Fig. 1) after TGFα treatment. These cells were invariably located at the distal ends of branches and may represent a subset of progenitor luminal cells (Pechoux et al., 1999;Shackleton et al., 2006). In untreated organoids, very few cells co-expressed K8 and K14 (1.4±0.2%; Supplemental Fig. 1). An examination of FGF7-treated or FGF7-TGFα dual-treated organoids revealed a similar orientation of myoepithelium to epithelium as that seen in TGFα-treated organoids (Fig. 6C, and data not shown), but fewer K8/K14 double positive cells were evident in the FGF7-treated compared to TGFα-treated organoids (Supplemental Fig. 1). Under all conditions, all organoids examined retained their central lumena. The developing branches also all contained lumena (Fig. 6).

FGF7 induces $MAPK^{ERK1,2}$ -dependent increase in K6-positive cells

K6-positive cells were previously shown to be localized to hyperproliferative areas in the mouse mammary gland and skin; this keratin has been considered a putative marker of stem/progenitor mouse mammary cells in some studies (Li et al., 2003; Welm et al., 2005). Since FGF7 induced sustained proliferation in the organoids, we asked whether it also induced higher numbers of K6-positive cells. Only a few K6-positive cells were evident in untreated and TGFα-treated organoids (Fig. 7A). When found, the K6-positive cells were rarely evident in the distal ends of branches and were found only at the base of branches (Figs. 7A, B). FGF7, alone or in combination with TGFα, induced a significant increase in the number of K6-positive cells compared to TGFα-treated organoids (Figs. 7A, B). Up-regulation of K6 expression occurred as early as 48 h after FGF7 stimulation (data not shown). The large numbers of K6-cells encapsulating the organoids were often found within the outer distal cell layers (Figs. 7A, B). We also noted that there were at least two populations of K6-positive cells in FGF7- or FGF7+TGFα-treated organoids: those that were $K6^+/K8^+$ and those that were basal $K6^+/K14^+$ (Fig. 7B; Supplemental Fig. 2 and Supplemental Fig. 3).

The FGF7-dependent effects also were $MAPK^{ERK1,2}$-dependent. Treatment with PD98059 prior to FGF7 or FGF7+TGFα stimulation inhibited both the increase in proliferation and the increase in the number of K6-positive cells in organoids stimulated with FGF7 (Fig. 7C; compare proliferation with 5C). As seen with TGFα-cultures, suppression of $MAPK^{ERK1,2}$ in FGF7-treated organoids also increased the number of dead cells close to the level of untreated controls (compare Fig. 7C with Fig. 5C).

Since FGF10 and FGF7 signal through a common isoform of FGFR2 referred to as FGFR2-iiib, we reasoned that many of the FGF7-associated phenotypes would be elicited also by FGF10. As expected, FGF10 failed to induce branching morphogenesis, inhibited TGFα-induced branching morphogenesis in a dose-dependent fashion, and up-regulated keratin-6 expression (Supplemental Fig. 4).

Discussion

Mammary branching morphogenesis requires exquisite time-dependent coordination of signaling between the ECM, hormones, and growth factors. It is not yet possible to do rapid time course and multifactorial analysis in vivo. Thus, despite intense study of the individual components, we know little about the precise signaling pathways, and the kinetics and mode of interactions among the different morphogenetic effectors. We developed a physiologically relevant, laminin-rich 3D assay where organoids from a few mice provide ample replicates and time points for such analysis.

We show that two growth factors produced by the mammary gland, TGFα and FGF7, induce very different outcomes in mammary organoids. A 1-h treatment with TGFα, followed by inhibition of $MAPK^{ERK1,2}$, was sufficient to induce a program of robust branching observed days later, whereas FGF7 treatment led to sustained growth and to formation of continuously growing cysts. We showed that whereas both factors signal through the $MAPK^{ERK1,2}$ pathway, TGFα stimulation leads to high levels of MEK1, $MAPK^{ERK1,2}$ phosphorylation for at least 1 h, while FGF7 induces a shorter duration (15 min) of phosphorylation. When the two factors are added together, the FGF7 $MAPK^{ERK1,2}$-dependent phenotype dominates and suppresses TGFα-induced branching (see Supplemental Movies 1–5).

Our data build upon the seminal work that found $MAPK^{ERK1,2}$ kinetics could determine the fate of PC12 cells cultured on conventional 2D plastic (Qui and Green, 1992; Traverse et al., 1992). These investigators found that EGF induced a rapid and transient induction of $MAPK^{ERK1,2}$ leading to cellular proliferation, while NGF induced a rapid but more prolonged phosphorylation, which in turn led to cellular differentiation. Therefore, a transient induction of $MAPK^{ERK1,2}$, in the one case with EGF added to PC12 cells and here with FGF7 added to mammary organoids, promotes proliferation. In contrast, a sustained activation of $MAPK^{ERK1,2}$ in PC12 with NGF promotes neuronal extension and in mammary organoids with TGFα leads to branching morphogenesis. The dominance of the FGF7-induced morphogenetic outcome in the mammary gland mediated through a transient activation of $MAPK^{ERK1,2}$ may be achieved through sustained activation of growth pathways.

We have published previously that amphiregulin is an important ligand for branching development of embryonic mammary tissue and that it signals through the stroma (Sternlicht et al., 2005). This ligand was also shown to be important for the branching morphogenesis that initiates at the onset of puberty in young female mice. However, it is not expressed in adult mammary gland tissue (Luetteke et al., 1999, and our unpublished data), the very tissue we are using in our study. There is strong evidence that in adult mice, branching occurs both during the estrous cycle and during gestation and primarily involves secondary or tertiary branching (Fata et al., 2001; Robinson et al., 2000; Atwood et al., 2000). Therefore, growth factors other than amphiregulin must regulate this morphogenetic process. We suggest that TGFα, which is expressed in adult mammary gland (Liscia et al., 1990), is a good candidate factor inducing morphogenesis during this time.

Transgenic overexpression of TGFα in epithelial cells of the mouse mammary gland induces extensive hyperplasia and occasional carcinoma (Matsui et al., 1990), and endogenously produced or exogenously added TGFα inhibits expression of whey acidic protein (WAP) in

primary mammary epithelial cells (Lin et al., 1995). Others have shown that expression of a dominant-negative EGFR in mammary epithelium inhibits ductal morphogenesis (Xie et al., 1997). These three studies indicate that TGFα is capable of acting directly on epithelial EGFR. However, transplantation studies and EGFR-null mammary tissue showed that signaling through stromal EGFR is required for extensive ductal outgrowth (Wiesen et al., 1999). Our current data suggest that exogenously added TGFα in this model system can induce signaling to epithelial EGFR and may mimic the stromal signaling required in vivo. It should be noted, however, that the branching seen in our organoids is more robust and exuberant than the spatially restricted branching seen in vivo in the mammary gland of virgin animals. We believe this is because in the 3D assay, the exogenous TGFα ligand is available to all the epithelial cells and leads to a global stimulation of the $MAPK^{ERK1,2}$ signal whereas *in vivo* there are likely discrete gradients of initiating or inhibitory signals, such as stromal TGFβ (Daniel et al., 1996; Nelson et al., 2006).

A possible explanation for the ability of TGFα to induce branching is that this growth factor induces two known morphogens, MMP-3 (Simian et al., 2001) and fibronectin (Sakai et al., 2003), and that these two factors are expressed in response to a prolonged activation of $MAPK^{ERK1,2}$. In other cell types in culture, mRNA expression of MMP-3 and fibronectin also was shown to be dependent on $MAPK^{ERK1,2}$ activation (Gaggioli et al., 2005; Park et al., 2004). Our previous and current data provide evidence that MMP-3 controls lateral branching in vivo (Wiseman et al., 2003) and is required for growth factor-induced mammary branching in type I collagen gels (Simian et al., 2001). Other MMPs may also be involved since complete inhibition of MMP activity with the broad based MMP inhibitor, GM6001, leads to a more drastic suppression of morphogenesis than inhibition of MMP-3 alone. Intriguingly, we found that inhibition of MMPs promotes continued lumen expansion. We had hypothesized that both down-regulation of MMP activity and apolar expression of the mammary morphogen, epimorphin, may play a role in formation of acinar lumen during late pregnancy and lactation (Hirai et al., 1998; Hirai et al., 2001). The data presented here indicate that FGF7 inhibits induction of MMP3. Thus, it would be interesting to investigate whether fibronectin is inhibited when epimorphin leads to lumen formation.

Fibronectin is a key factor regulating branching in a number of organs including the salivary gland (Larsen et al., 2006; Sakai et al., 2003). Here we show that this ECM molecule also participates in branching in the mammary gland. Inhibition of the fibronectin receptor (α5β1) using blocking antibodies leads to altered morphogenesis where branch extensions are reduced and development verges on abnormal growth. The ability of FGF7 to suppress fibronectin expression may thus be an important reason for its ability to be dominant over TGFα‘s ability to induce branching.

It is intriguing that both TGFα and FGF7 changed the profile of the keratin-expressing cells and stimulated two different progenitor cell populations. Whereas TGFα induced an increase in $K8^+/K14^+$ cells, FGF7 increased the number of $K8^+/K6^+$ and $K14^+/K6^+$-positive cells. The $K8^+/K14^+$ (similar to $K19^+/K14^+$) cell-type has been suggested to represent luminal progenitor cells (Gudjonsson et al., 2002; Shackleton et al., 2006). Interestingly, cells double positive for $K8^+/K14^+$ are the majority cell type in embryonic urogenital sinus epithelium and the developing prostatic epithelium and are considered progenitor/stem cells within these tissues (Wang et al., 2001). In mammary epithelium, $K8^-/K14^+$ cells, which represent the myoepithelial population, can be derived from the $K8^+/K14^-$ luminal epithelium (Pechoux et al., 1999). The importance of myoepithelial cells in mammary gland biology and breast cancer has received recent attention (Adriance et al., 2005; Faraldo et al., 2005). Aside from myoepithelial cells being important for milk ejection, they have been shown to act also as natural tumor suppressors which can establish or maintain acini polarity (Gudjonsson et al., 2002). It may be reasonable to hypothesize that in the absence of functional myoepithelial cells,

branching morphogenesis would likely not occur properly. Specific ablation of either myoepithelial function or myoepithelial cells as a whole could address this hypothesis and conditional gene targeting could be used, as it has previously, as an in vivo approach to better understand the many functions these cells appear to execute (Faraldo et al., 2005).

A previous study using our assay and organoids from embryonic (e18.5) mammary glands showed that FGF7 did in fact induce branching morphogenesis (Sternlicht et al., 2005). The explanation lies in the fact that at different stages of mammary gland development, the composition of the ligands and the receptors change, i.e. this is an age-dependent phenomenon. A comparison of organoids from these two different age groups (embryonic vs. 10–14 weeks old) in the same mouse background in the same experiment confirmed that the response of mammary epithelium to FGF7 in 3D cultures is dependent on the age of the donor mouse (unpublished results). In this report, we used organoids from adult (10–14 weeks old) mammary glands, and under these conditions, FGF7 not only fails to induce branching but also inhibits TGFα-induced morphogenesis pointing to the exquisite, stage- and time-dependent changes that occur in the mammary gland as it develops after birth. Indeed, expression of both mammary epithelial FGF7 receptor and stromal FGF7 has been shown to be developmentally regulated (Coleman-Krnacik and Rosen, 1994; Mailleux et al., 2002; Pedchenko and Imagawa, 2000), suggesting that the ratio of ligand to receptor may be one important reason for the altered morphogenetic outcome.

FGF7-dependent phenotypes were dependent on a transient induction of $MAPK^{ERK1,2}$ since both proliferation and expansion of K6-positve cells by FGF7 were inhibited completely by PD98059. $K6^{+}$ cells were shown to localize to hyperproliferative areas in Wnt-1 tumors and terminal end buds within the mouse mammary gland and were proposed also to represent a marker for stem/progenitor mouse mammary cells (Li et al., 2003; Welm et al., 2005). Recently, a sub-population of mammary epithelial cells having high levels of the stem cell marker Sca-1, and displaying properties of mammary stem/progenitor cells, were found to be primarily K6 positive (Deugnier et al., 2006). However, mammary glands examined from K6-embryonic knockout mice revealed that this keratin may not be necessary for ductal development, possibly arguing against K6 as a functional molecule for maintenance of the stem/progenitor cell population in the mammary gland (Grimm et al., 2006). The exact mechanism by which FGF7 induces K6 expression while TGFα does not remains to be elucidated. The difference between these two growth factors may lie in their ability to induce distinct transcription factors. For instance, in the development of the *Drosophila* air sac, which requires both FGF and EGF signaling, the ets domain transcription factor, Pointed (downstream of $MAPK^{ERK1,2}$ activation) is needed for branchless/FGF-induced cell migration but dispensable for EGF-induced cell proliferation/survival (Cabernard and Affolter, 2005). Although the development of the *Drosophila* trachea is quite different from branching morphogenesis in the mouse mammary gland, the conserved signalling cascades have given insights into the mechanisms of how different growth factors elicit different morphogenetic responses within the same tissue.

FGF10 mimicked several of the phenotypes induced by FGF7, which is consistent with the report that these two growth factors signal through the common receptor FGFR2-iiib. Both FGF10 and FGFR2-iiib have been shown to be necessary for mammary placode/ductal development during embryogenesis (Mailleux et al., 2002). FGF7-null mice are at least capable of lactation (Guo et al., 1996), indicating that FGF7 may not be necessary for functional lobulo-alveolar morphogenesis. However, to our knowledge there has not been a complete analysis of the female mammary gland isolated from FGF7-null female mice—leaving it an open question as to whether this growth factor is or is not important for mammary branching morphogenesis *in vivo*.

We are currently investigating how FGF7 may antagonize TGFα-induced signalling and morphogenesis. This antagonism would prove difficult to study in the complex in vivo environment, which could possibly explain the absence of previous reports on this interesting finding. Our initial efforts have focussed on determining the localization of the receptors for TGFα and FGF7 (EGFR and FGFR2 respectively) in organoids. These efforts have identified an apparent spatial difference found within the myoepithelial compartment. Specifically, FGFR2 is abundant within myoepithelial cells while EGFR is restricted to a few myoepithelial cells/organoid (Supplemental Fig. 5). Within the luminal epithelial compartment, both EGFR and FGFR2 appear to be distributed homogeneously in all cells. Therefore, FGF7 may antagonize TGFα-induced signalling and morphogenesis directly in luminal cells (and the few myoepithelial cells that contain both EGFR and FGFR2) as well as indirectly by modulating those myoepithelial cells that lack EGFR. The latter process would involve a mechanism independent of regulating $MAPK^{ERK1,2}$ activation. Alterations in these two compartments would affect morphogen expression and cell–cell communication that together may override TGFα-induced morphogenesis. How FGF7 antagonizes TGFα activation of $MAPK^{ERK1,2}$ could involve mechanisms that include augmenting EGFR receptor turnover through FGF7-activation of the ubiquitin ligase Cbl (Schlessinger, 2004), increasing MAPK phosphatase activity, and/or inhibiting induction of RAP1 which has been shown to sustain $MAPK^{ERK1,2}$ activation (York et al., 1998). Whereas we cannot be certain that the TGFα-and FGF7-associated phenotypes are solely dependent on $MAPK^{ERK1,2}$ activation, our data clearly indicate that distinct activation kinetics are associated with distinct phenotypes.

In summary, we find that phosphorylation of $MAPK^{ERK1,2}$ and duration of its activation are directly related to outcome in the organotypic 3D primary culture system we have developed to study mammary gland branching morphogenesis. We find that the interplay between the different growth factors, their spatial localization, and the duration of their activation as well as downstream effectors such as MMP-3 and fibronectin cooperate and choreograph whether mammary branches initiate and elongate. Finally, the interplay between TGFα and FGF7 suggests that the mammary epithelium integrates multiple and simultaneously delivered growth factor signals in part, at the level of the duration of the $MAPK^{ERK1,2}$ signal. It will be informative to develop genetic mouse models where $MAPK^{ERK1,2}$ activation kinetics could be precisely controlled within the mammary gland to test whether or not the kinetics of $MAPK^{ERK1,2}$ activation is the sole determinant for the morphogenetic outcomes observed.

Supplementary Material

Refer to Web version on PubMed Central for supplementary material.

Acknowledgments

This work was supported by grants from the United States Department of Energy, Office of Biological and Environmental Research (DEAC0376SF00098) to MJB, the National Cancer Institute (CA57621) to ZW, and MJB and a grant (ES012801) to ZW jointly funded by the National Institute of Environmental Health Sciences and National Cancer Institute. JEF was supported, in part, by the California Breast Cancer Research Program (FB-0131) and by the Department of Defense Breast Cancer Research Program (DAMD17-03-1-0486). HM was supported by the Susan G. Komen Breast Cancer Foundation (02-1591). AJE was supported by NIH Grant number HL-007731 (NRSA Institutional Fellowship) and by the California Breast Cancer Research Program (11FB-0015). MJB is the recipient of both an Innovator award from the DOD Breast Cancer Program and a Distinguished Fellowship in Life Sciences from the OBER Office of the US DOE. The time-lapse microscopy was done using equipment from the UCSF Comprehensive Cancer Center LCA Core. We also thank Andy Finch for assistance in developing time-lapse microscope automations in OpenLab.

References

Adriance MC, Inman JL, Petersen OW, Bissell MJ. Myoepithelial cells: good fences make good neighbors. Breast Cancer Res 2005;7:190–197. [PubMed: 16168137]

Atwood CS, Hovey RC, Glover JP, Chepko G, Ginsburg E, Robison WG, Vonderhaar BK. Progesterone induces side-branching of the ductal epithelium in the mammary glands of peripubertal mice. J. Endocrinol 2000;167:39–52. [PubMed: 11018751]

Ballif BA, Blenis J. Molecular mechanisms mediating mammalian mitogen-activated protein kinase (MAPK) kinase (MEK)-MAPK cell survival signals. Cell Growth Differ 2001;12:397–408. [PubMed: 11504705]

Cabernard C, Affolter M. Distinct roles for two receptor tyrosine kinases in epithelial branching morphogenesis in *Drosophila*. Dev. Cell 2005;9:831–842. [PubMed: 16326394]

Coleman-Krnacik S, Rosen JM. Differential temporal and spatial gene expression of fibroblast growth factor family members during mouse mammary gland development. Mol. Endocrinol 1994;8:218–229. [PubMed: 8170478]

Corson LB, Yamanaka Y, Lai KM, Rossant J. Spatial and temporal patterns of ERK signaling during mouse embryogenesis. Development 2003;130:4527–4537. [PubMed: 12925581]

Daniel CW, Robinson S, Silberstein GB. The role of TGF-beta in patterning and growth of the mammary ductal tree. J. Mammary Gland Biol. Neoplasia 1996;1:331–341. [PubMed: 10887507]

Deugnier MA, Faraldo MM, Teuliere J, Thiery JP, Medina D, Glukhova MA. Isolation of mouse mammary epithelial progenitor cells with basal characteristics from the Comma-Dbeta cell line. Dev. Biol 2006;293:414–425. [PubMed: 16545360]

Emerman JT, Vogl AW. Cell size and shape changes in the myoepithelium of the mammary gland during differentiation. Anat. Rec 1986;216:405–415. [PubMed: 3789423]

Faraldo MM, Teuliere J, Deugnier MA, Taddei-De La Hosseraye I, Thiery JP, Glukhova MA. Myoepithelial cells in the control of mammary development and tumorigenesis: data from genetically modified mice. J. Mammary Gland Biol. Neoplasia 2005;10:211–219. [PubMed: 16807801]

Fata JE, Chaudhary V, Khokha R. Cellular turnover in the mammary gland is correlated with systemic levels of progesterone and not 17beta-estradiol during the estrous cycle. Biol. Reprod 2001;65:680–688. [PubMed: 11514328]

Fata JE, Werb Z, Bissell MJ. Regulation of mammary gland branching morphogenesis by the extracellular matrix and its remodeling enzymes. Breast Cancer Res 2004;6:1–11. [PubMed: 14680479]

Gaggioli C, Deckert M, Robert G, Abbe P, Batoz M, Ehrengruber MU, Ortonne JP, Ballotti R, Tartare-Deckert S. HGF induces fibronectin matrix synthesis in melanoma cells through MAP kinase-dependent signaling pathway and induction of Egr-1. Oncogene 2005;24:1423–1433. [PubMed: 15608673]

Grimm SL, Bu W, Longley MA, Roop DR, Li Y, Rosen JM. Keratin 6 is not essential for mammary gland development. Breast Cancer Res 2006;8:R29. [PubMed: 16790075]

Gudjonsson T, Villadsen R, Nielsen HL, Ronnov-Jessen L, Bissell MJ, Petersen OW. Isolation, immortalization, and characterization of a human breast epithelial cell line with stem cell properties. Genes Dev 2002;16:693–706. [PubMed: 11914275]

Guo L, Degenstein L, Fuchs E. Keratinocyte growth factor is required for hair development but not for wound healing. Genes Dev 1996;10:165–175. [PubMed: 8566750]

Hida M, Omori S, Awazu M. ERK and p38 MAP kinase are required for rat renal development. Kidney Int 2002;61:1252–1262. [PubMed: 11918731]

Hirai Y, Lochter A, Galosy S, Koshida S, Niwa S, Bissell MJ. Epimorphin functions as a key morphoregulator for mammary epithelial cells. J. Cell Biol 1998;140:159–169. [PubMed: 9425164]

Hirai Y, Radisky D, Boudreau R, Simian M, Stevens ME, Oka Y, Takebe K, Niwa S, Bissell MJ. Epimorphin mediates mammary luminal morphogenesis through control of C/EBPbeta. J. Cell Biol 2001;153:785–794. [PubMed: 11352939]

Hovey RC, Trott JF, Vonderhaar BK. Establishing a framework for the functional mammary gland: from endocrinology to morphology. J. Mammary Gland Biol. Neoplasia 2002;7:17–38. [PubMed: 12160083]

Karihaloo A, Kale S, Rosenblum ND, Cantley LG. Hepatocyte growth factor-mediated renal epithelial branching morphogenesis is regulated by glypican-4 expression. Mol. Cell. Biol 2004;24:8745–8752. [PubMed: 15367691]

Kashimata M, Sayeed S, Ka A, Onetti-Muda A, Sakagami H, Faraggiana T, Gresik EW. The ERK-1/2 signaling pathway is involved in the stimulation of branching morphogenesis of fetal mouse submandibular glands by EGF. Dev. Biol 2000;220:183–196. [PubMed: 10753509]

Kling DE, Lorenzo HK, Trbovich AM, Kinane TB, Donahoe PK, Schnitzer JJ. MEK-1/2 inhibition reduces branching morphogenesis and causes mesenchymal cell apoptosis in fetal rat lungs. Am. J. Physiol.: Lung Cell. Mol. Physiol 2002;282:L370–L378. [PubMed: 11839529]

Larsen M, Wei C, Yamada KM. Cell and fibronectin dynamics during branching morphogenesis. J. Cell Sci 2006;119:3376–3384. [PubMed: 16882689]

Li Y, Welm B, Podsypanina K, Huang S, Chamorro M, Zhang X, Rowlands T, Egeblad M, Cowin P, Werb Z, Tan LK, Rosen JM, Varmus HE. Evidence that transgenes encoding components of the Wnt signaling pathway preferentially induce mammary cancers from progenitor cells. Proc. Natl. Acad. Sci. U. S. A 2003;100:15853–15858. [PubMed: 14668450]

Lin CQ, Dempsey PJ, Coffey RJ, Bissell MJ. Extracellular matrix regulates whey acidic protein gene expression by suppression of TGF-alpha in mouse mammary epithelial cells: studies in culture and in transgenic mice. J. Cell. Biol 1995;129:1115–1126. [PubMed: 7744960]

Liscia DS, Merlo G, Ciardiello F, Kim N, Smith GH, Callahan R, Salomon DS. Transforming growth factor-alpha messenger RNA localization in the developing adult rat and human mammary gland by in situ hybridization. Dev. Biol 1990;140:123–131. [PubMed: 2358112]

Luetteke NC, Qiu TH, Fenton SE, Troyer KL, Riedel RF, Chang A, Lee DC. Targeted inactivation of the EGF and amphiregulin genes reveals distinct roles for EGF receptor ligands in mouse mammary gland development. Development 1999;126:2739–2750. [PubMed: 10331984]

Mailleux AA, Spencer-Dene B, Dillon C, Ndiaye D, Savona-Baron C, Itoh N, Kato S, Dickson C, Thiery JP, Bellusci S. Role of FGF10/FGFR2b signaling during mammary gland development in the mouse embryo. Development 2002;129:53–60. [PubMed: 11782400]

Maroun CR, Holgado-Madruga M, Royal I, Naujokas MA, Fournier TM, Wong AJ, Park M. The Gab1 PH domain is required for localization of Gab1 at sites of cell-cell contact and epithelial morphogenesis downstream from the met receptor tyrosine kinase. Mol. Cell. Biol 1999;19:1784–1799. [PubMed: 10022866]

Marshall CJ. Specificity of receptor tyrosine kinase signaling: transient versus sustained extracellular signal-regulated kinase activation. Cell 1995;80:179–185. [PubMed: 7834738]

Matsui Y, Halter SA, Holt JT, Hogan BL, Coffey RJ. Development of mammary hyperplasia and neoplasia in MMTV-TGF alpha transgenic mice. Cell 1990;61:1147–1155. [PubMed: 2161707]

Nelson CM, Dujin M, Inman JL, Fletcher DA, Bissell MJ. Tissue geometry determines sites of mammary branching morphogenesis in organotypic cultures. Science 2006;314:298–300. [PubMed: 17038622]

Park CH, Lee MJ, Ahn J, Kim S, Kim HH, Kim KH, Eun HC, Chung JH. Heat shock-induced matrix metalloproteinase (MMP)-1 and MMP-3 are mediated through ERK and JNK activation and via an autocrine interleukin-6 loop. J. Invest. Dermatol 2004;123:1012–1019. [PubMed: 15610507]

Parmar H, Cunha GR. Epithelial–stromal interactions in the mouse and human mammary gland in vivo. Endocr. Relat. Cancer 2004;11:437–458. [PubMed: 15369447]

Pechoux C, Gudjonsson T, Ronnov-Jessen L, Bissell MJ, Petersen OW. Human mammary luminal epithelial cells contain progenitors to myoepithelial cells. Dev. Biol 1999;206:88–99. [PubMed: 9918697]

Pedchenko VK, Imagawa W. Pattern of expression of the KGF receptor and its ligands KGF and FGF-10 during postnatal mouse mammary gland development. Mol. Reprod. Dev 2000;56:441–447. [PubMed: 10911393]

Qui MS, Green SH. PC12 cell neuronal differentiation is associated with prolonged p21ras activity and consequent prolonged ERK activity. Neuron 1992;9:705–717. [PubMed: 1382473]

Robinson GW, Hennighausen L, Johnson PF. Side-branching in the mammary gland: the progesterone-Wnt connection. Genes Dev 2000;14:889–894. [PubMed: 10783160]

Roux PP, Blenis J. ERK and p38 MAPK-activated protein kinases: a family of protein kinases with diverse biological functions. Microbiol. Mol. Biol. Rev 2004;68:320–344. [PubMed: 15187187]

Sakai T, Larsen M, Yamada KM. Fibronectin requirement in branching morphogenesis. Nature 2003;423:876–881. [PubMed: 12815434]

Schedin P, Mitrenga T, McDaniel S, Kaeck M. Mammary ECM composition and function are altered by reproductive state. Mol. Carcinog 2004;41:207–220. [PubMed: 15468292]

Schlessinger J. Common and distinct elements in cellular signaling via EGF and FGF receptors. Science 2004;306:1506–1507. [PubMed: 15567848]

Shackleton M, Vaillant F, Simpson KJ, Stingl J, Smyth GK, Asselin-Labat ML, Wu L, Lindeman GJ, Visvader JE. Generation of a functional mammary gland from a single stem cell. Nature 2006;439:84–88. [PubMed: 16397499]

Simian M, Hirai Y, Navre M, Werb Z, Lochter A, Bissell MJ. The interplay of matrix metalloproteinases, morphogens and growth factors is necessary for branching of mammary epithelial cells. Development 2001;128:3117–3131. [PubMed: 11688561]

Sternlicht MD. Key stages in mammary gland development: the cues that regulate ductal branching morphogenesis. Breast Cancer Res 2006;8:201. [PubMed: 16524451]

Sternlicht MD, Sunnarborg SW, Kouros-Mehr H, Yu Y, Lee DC, Werb Z. Mammary ductal morphogenesis requires paracrine activation of stromal EGFR via ADAM17-dependent shedding of epithelial amphiregulin. Development 2005;132:3923–3933. [PubMed: 16079154]

Traverse S, Gomez N, Paterson H, Marshall C, Cohen P. Sustained activation of the mitogen-activated protein (MAP) kinase cascade may be required for differentiation of PC12 cells. Comparison of the effects of nerve growth factor and epidermal growth factor. Biochem. J 1992;288(Pt 2):351–355. [PubMed: 1334404]

Wang Y, Hayward S, Cao M, Thayer K, Cunha G. Cell differentiation lineage in the prostate. Differentiation 2001;68:270–279. [PubMed: 11776479]

Weaver VM, Lelievre S, Lakins JN, Chrenek MA, Jones JC, Giancotti F, Werb Z, Bissell MJ. beta4 integrin-dependent formation of polarized three-dimensional architecture confers resistance to apoptosis in normal and malignant mammary epithelium. Cancer Cell 2002;2:205–216. [PubMed: 12242153]

Welm AL, Kim S, Welm BE, Bishop JM. MET and MYC cooperate in mammary tumorigenesis. Proc. Natl. Acad. Sci. U. S. A 2005;102:4324–4329. [PubMed: 15738393]

Wiesen JF, Young P, Werb Z, Cunha GR. Signaling through the stromal epidermal growth factor receptor is necessary for mammary ductal development. Development 1999;126:335–344. [PubMed: 9847247]

Wiseman BS, Sternlicht MD, Lund LR, Alexander CM, Mott J, Bissell MJ, Soloway P, Itohara S, Werb Z. Site-specific inductive and inhibitory activities of MMP-2 and MMP-3 orchestrate mammary gland branching morphogenesis. J. Cell Biol 2003;162:1123–1133. [PubMed: 12975354]

Xie W, Paterson AJ, Chin E, Nabell LM, Kudlow JE. Targeted expression of a dominant negative epidermal growth factor receptor in the mammary gland of transgenic mice inhibits pubertal mammary duct development. Mol. Endocrinol 1997;11:1766–1781. [PubMed: 9369445]

York RD, Yao H, Dillon T, Ellig CL, Eckert SP, McCleskey EW, Stork PJ. Rap1 mediates sustained MAP kinase activation induced by nerve growth factor. Nature 1998;392:622–626. [PubMed: 9560161]

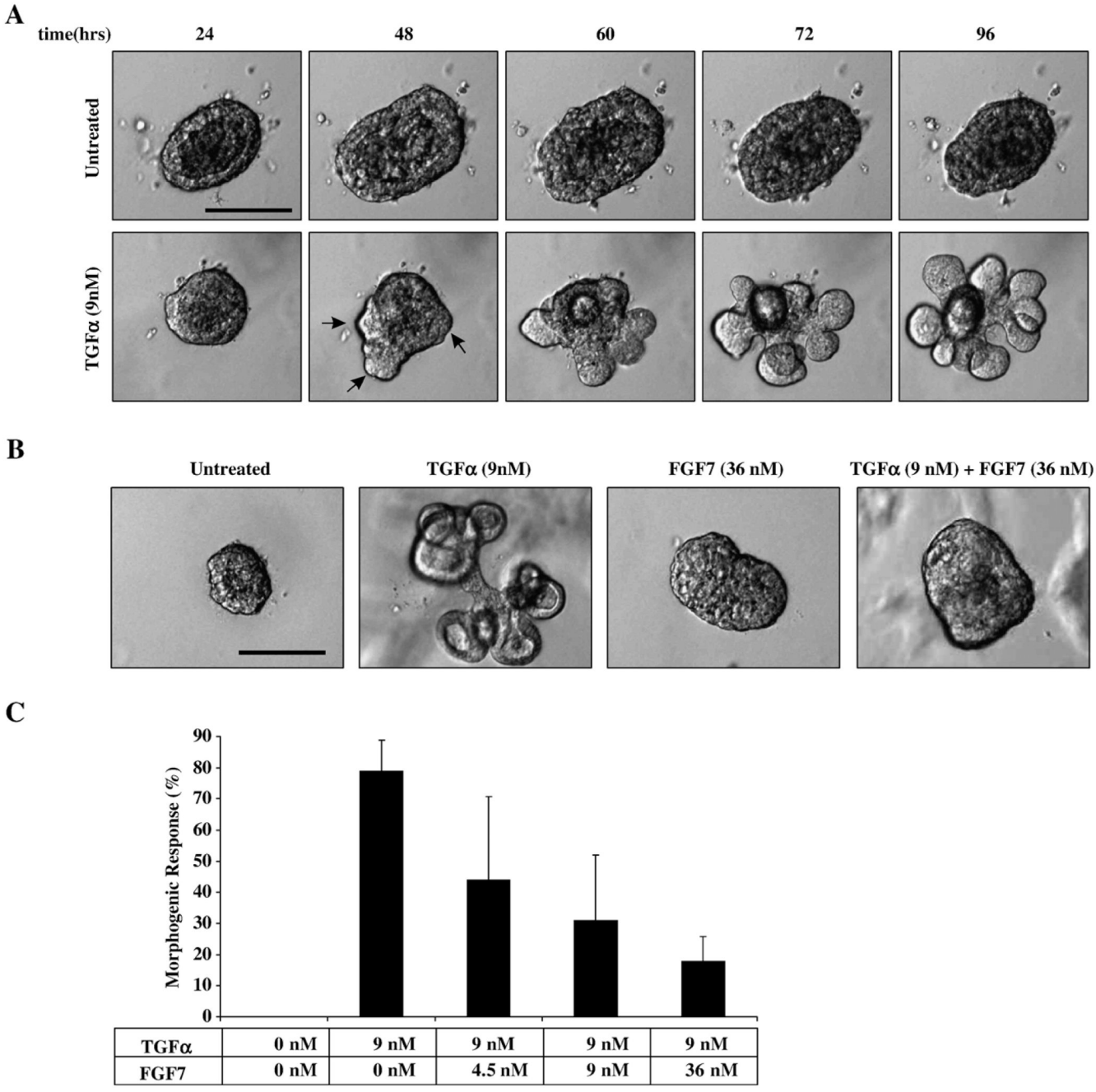

Fig. 1.

Organoid response to TGFα and FGF7. (A) Untreated organoids fail to undergo major morphological changes, except a slight lumen expansion followed by compression from 48 to 60 h. In contrast, TGFα stimulation initiates bud formation (arrows) within 48 h, with the majority of morphogenesis occurring within the 48- to 72-h window. Images represent frames taken from movies (Supplemental Movies 1 and 2). (B, C) FGF7 fails to induce branching morphogenesis and suppresses TGFα-induced morphogenesis in a dose-dependent manner. Please see Supplemental Movies 3 and 4. (C) Morphometric analysis of branching morphogenesis. Scale bars represent 100 μm. Data are represented as mean morphogenetic

response±standard deviation (SD) and involve counting at least 100 organoids per condition per experiment.

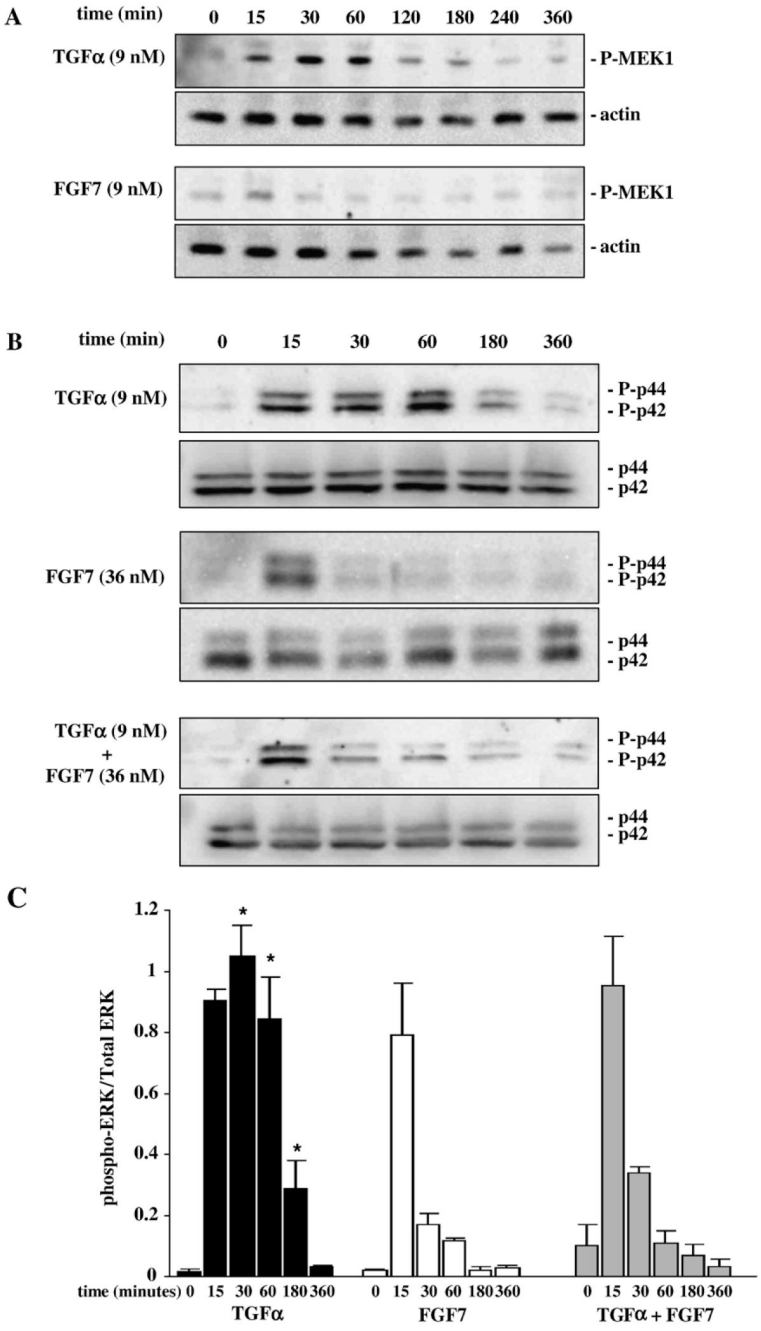

Fig. 2.

FGF7 attenuates TGFα-induced MAPK^{ERK1,2} activation. (A, B) Activation of high MEK1 (P-MEK1) and MAPK^{ERK1,2} (P-p44, P-p42) levels are sustained for 1 h in organoids stimulated with TGFα compared to only 15 min in organoids stimulated with FGF7. Actin and total MAPK^{ERK1,2} (p44, p42) are provided as loading controls. (B) FGF7 attenuates TGFα activation of MAPK^{ERK1,2} when the growth factors are added simultaneously to the organoids. (C) Quantitative analysis of MAPK^{ERK1,2} activation: MAPK^{ERK1,2} activation in organoids treated with TGFα is significantly different than those treated with FGF7 *[p <0.05], or those treated with FGF7 plus TGFα at 30, 60, and 180 min. Data are represented as the mean of phospho-MAPK^{ERK1,2} levels/total MAPK^{ERK1,2} ±standard deviation (SD).

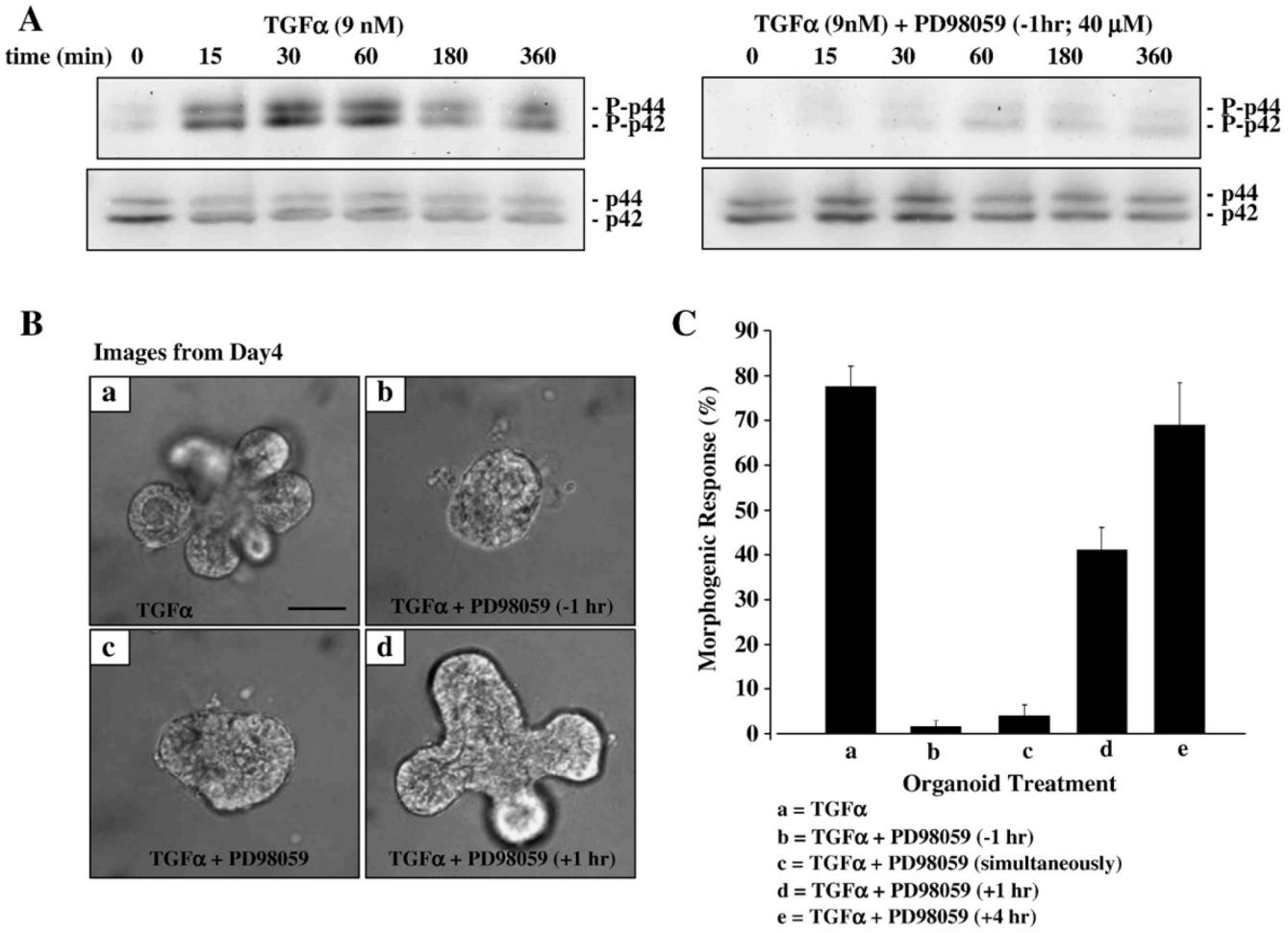

Fig. 3.

One hour of MAPK^{ERK1,2} activation is necessary and sufficient for TGFα-induced morphogenesis. (A) TGFα induces a rapid increase in active MAPK^{ERK1,2} activation. PD98059, the MEK inhibitor, suppresses TGFα-induced MAPK^{ERK1,2} activation when added 1 h before TGFα stimulation. Active MAPK^{ERK1,2} (P-p44/P-p42) and total MAPK^{ERK1,2} (p44/p42) were visualized on the same membrane in each condition. Membranes were transferred and developed simultaneously. (B) (a) TGFα alone. Pre-treatment with PD98059 for 1 h (b), or simultaneous addition with TGFα at time 0 h (c), completely inhibits morphogenesis (see the Supplemental Movie 5). Addition of PD98059 at 1 h (d) or 4 h (not shown) after TGFα treatment fails to inhibit morphogenesis completely. (C) Quantification of the percentage of organoids undergoing a morphogenetic response similar to TGFα-treated samples (a=untreated, b=PD98059 pre-treatment followed by TGFα, c=TGFα+PD98059 added simultaneously, d=PD98059 added after 1 h of TGFα stimulation, e=PD98059 added after 4 h of TGFα stimulation). Scale bar equals 50 μm. Data are represented as mean morphogenetic response±SD and involve counting at least 100 organoids per condition per experiment.

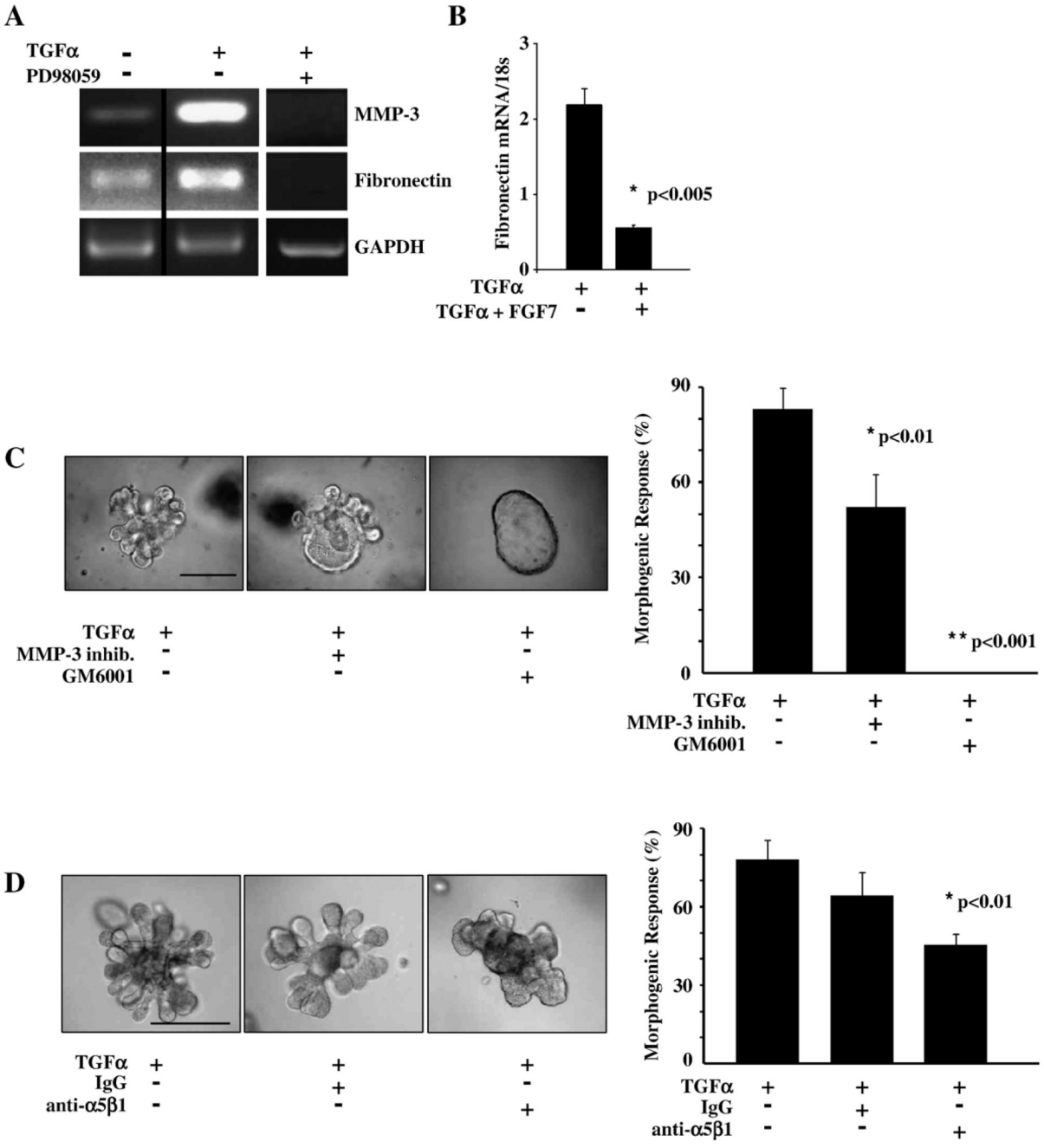

Fig. 4.

Inhibition of MMP-3 activity and fibronectin adhesion alters TGFα-induced morphogenesis. (A) TGFα induces MAPK^{ERK1,2}-dependent mRNA expression of MMP-3 and fibronectin. (B) FGF7 inhibits TGFα-induced expression of fibronectin mRNA levels (quantitative PCR). Data are represented as the mean ratio of fibronectin mRNA/18s±SD. (C) A peptide-based inhibitor specific to MMP-3 (20 μM) or the general metalloproteinase inhibitor, GM6001 (40 μM) suppresses morphogenesis and often leads to formation of cyst-like structures. (D) Addition of a blocking antibody (2 μg/ml) against the fibronectin receptor, α5β1 integrin alters morphogenesis, while a non-specific isotype IgG antibody (2 μg/ml) has no effect. Quantification represents the percentage of structures undergoing morphogenesis under

different conditions. Data are represented as mean morphogenetic response±SD and involve counting at least 100 organoids per condition per experiment. Scale bars in panels C and D equal 200 μm.

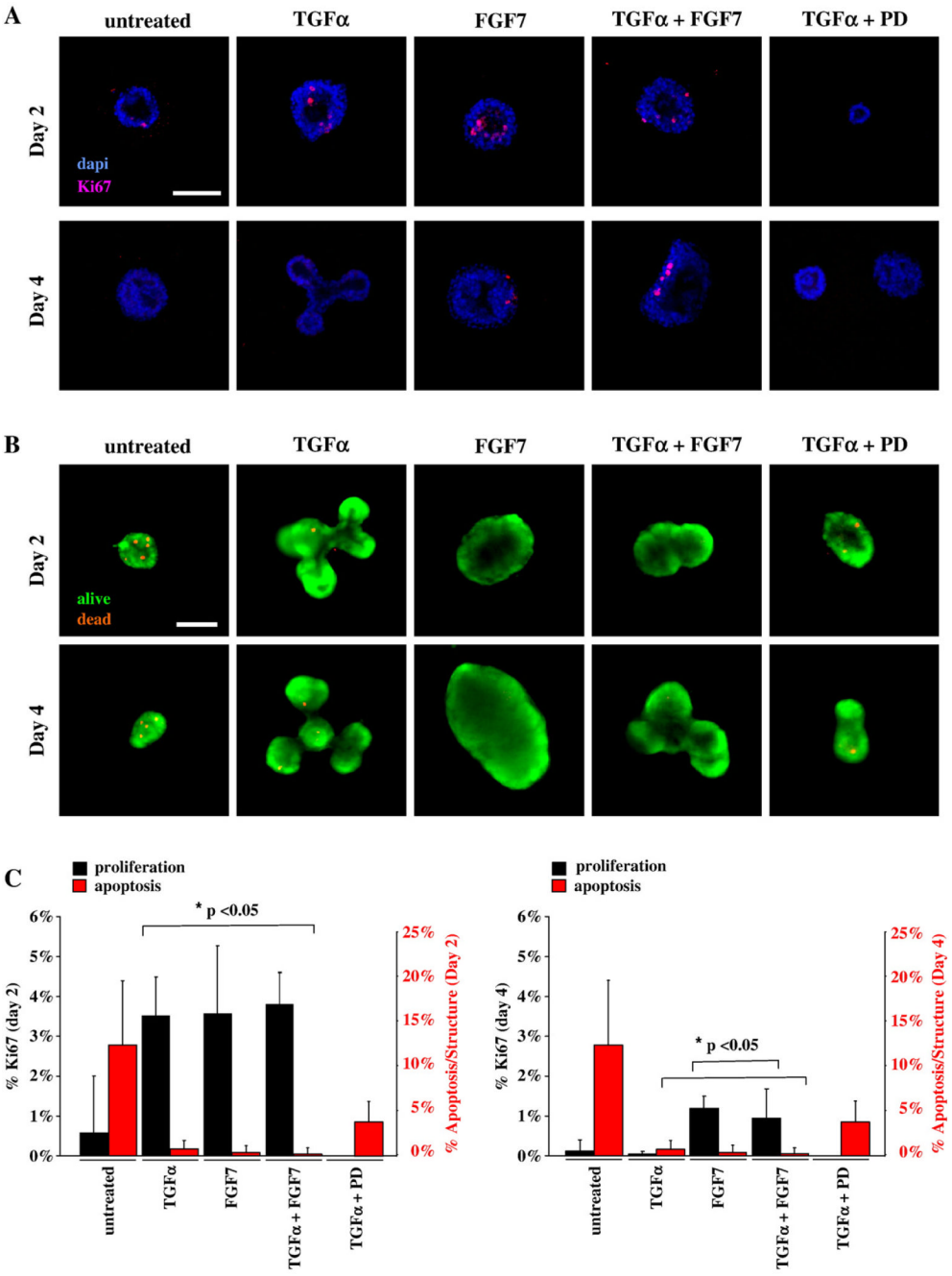

Fig. 5.

MAPK^{ERK1,2} regulates organoid proliferation and apoptosis. (A) TGFα-induced proliferation (determined by Ki67 immunocytochemistry with DAPI counter stain for nuclei) is inhibited by PD98059 but augmented by FGF7. (B) Live cells are labeled with the vital dye Calcein AM (green) and dead cells are labeled with ethidium homodimer-1 (orange). Dead cells are prevalent in untreated and PD98059-treated organoids. (C) Organoids treated with FGF7 show continued proliferation on day 4. (C) TGFα plus PD98059-treated and control organoids analyzed at day 2 or day 4 have significantly higher apoptosis than those treated with TGFα or FGF7. *Significantly different than all other conditions. Scale bars equal 50 μm. Data are

represented as mean percent Ki67±SD and mean percent apoptosis±SD and involve counting at least 10 randomly selected organoids per condition per experiment.

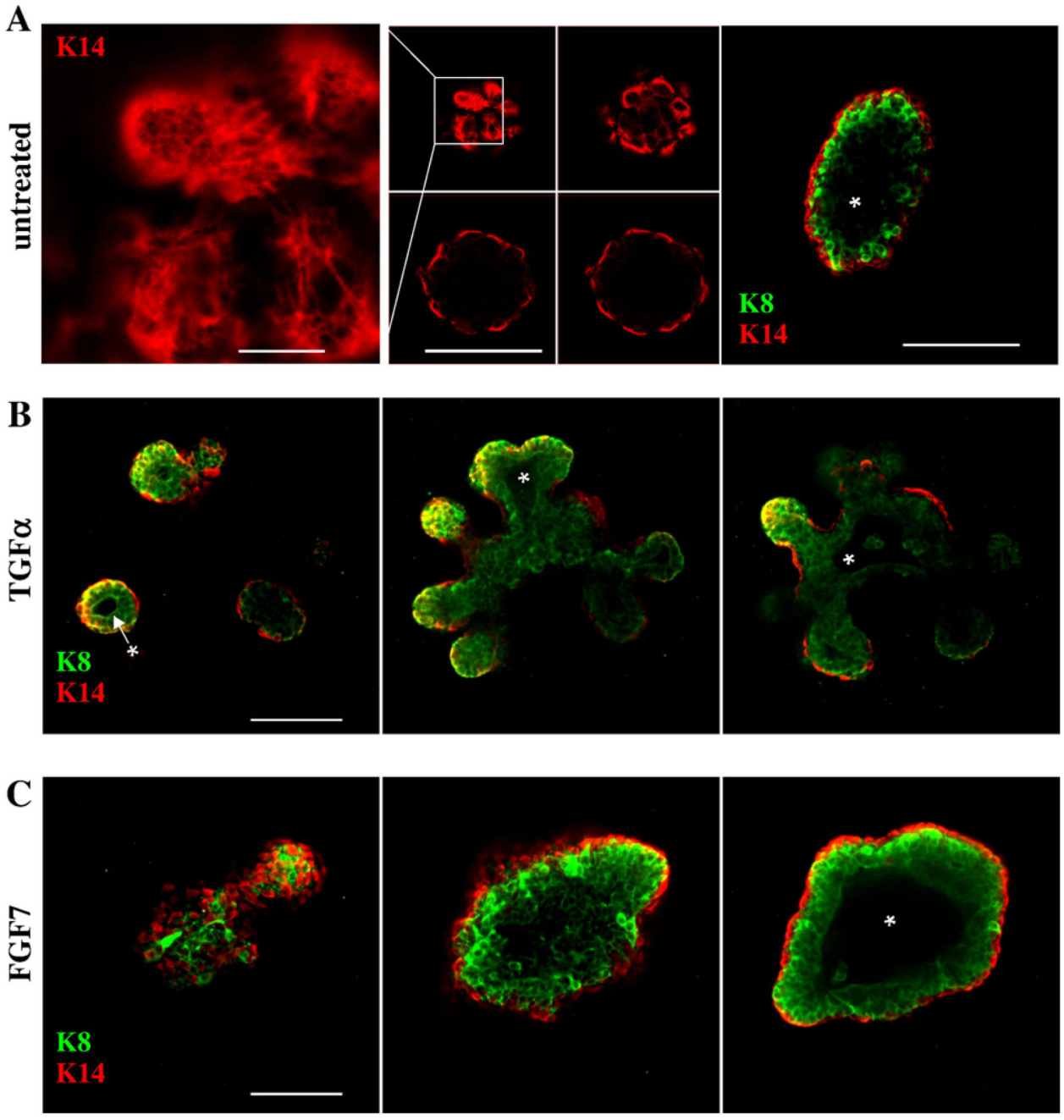

Fig. 6.

Orientation of myoepithelial and epithelial cells is maintained in organoids undergoing morphogenesis. Indirect immunofluorescence for K14 (red; myoepithelium) and K8 (green; epithelium) in cultured organoids was captured by confocal microscopy. (A–C) Epithelial cells are the small tightly packed cuboidal cells. Myoepithelial cells are the larger cells displaying membrane extensions; they retain their basal orientation with respect to epithelial cells. (A) Untreated organoids, day 4. (B) TGFα-treated organoids, day 4. (C) FGF7-treated organoids, day 4. A montage of merged K8/K14 confocal stacks is represented in panels B and C and indicate that cells at the distal ends of branches in panel B are K8/K14 double positive (yellow

signal). Lumena (*) are evident in all structures treated with TGFα or FGF7. Scale bars in panel A equal 5 μm (left panel) and 50 μm (right panels). Scale bars in panels B and C equal 50 μm.

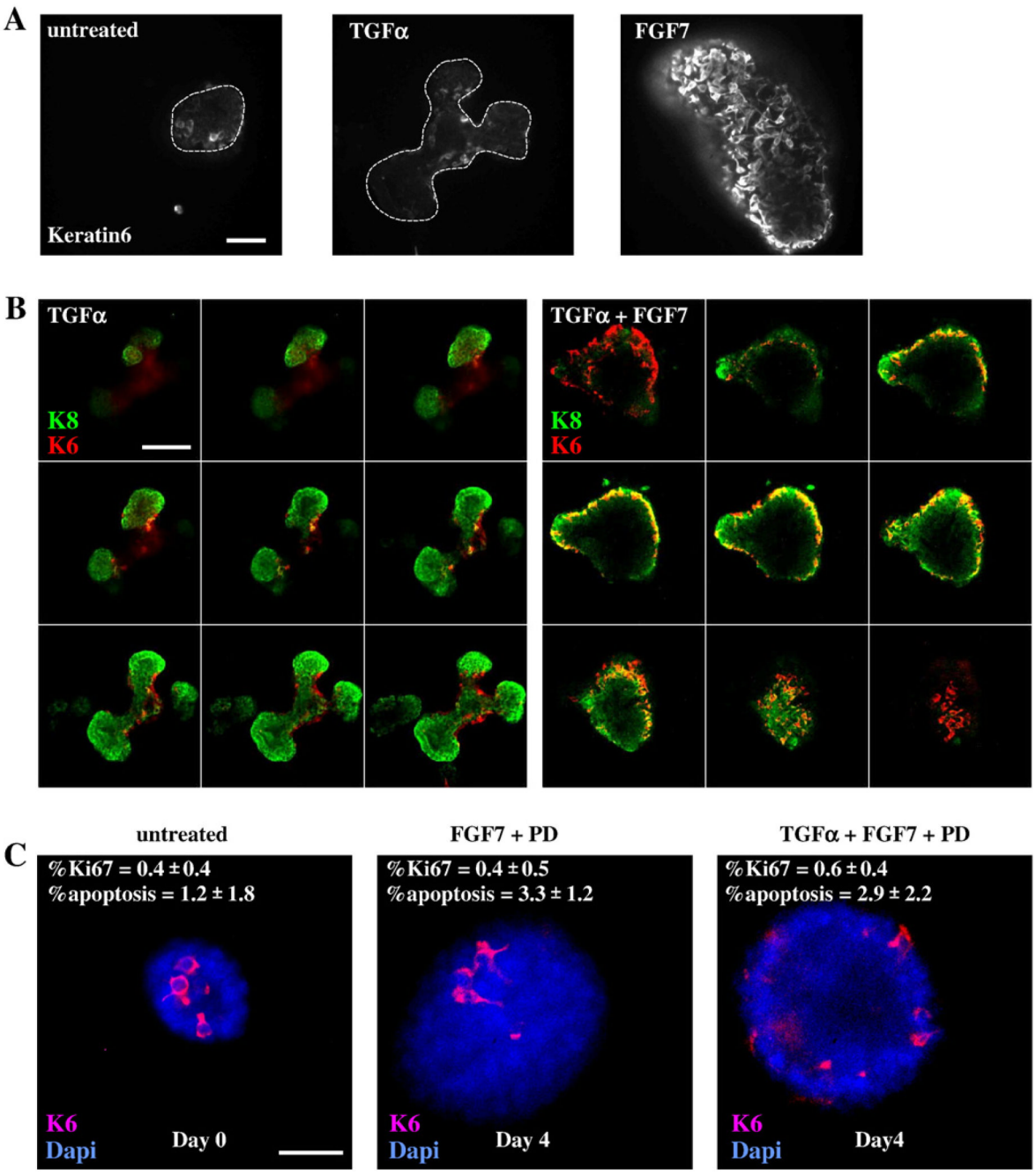

Fig. 7.

FGF7 induces MAPK^{ERK1,2}-dependent increase in K6-positive cells as well as organoid proliferation. (A) FGF7-induced K6-positive cells are evident on the outside of the organoid (day 4). (B) K6-positive cells in TGFα-treated organoids remain at the base of the branch, while K6-positive cells in FGF7-treated organoids are found both encapsulating and within the organoid. Some of these K6-positive cells are K8/K6 double positive (yellow). (C) FGF7-induced proliferation and increase in K6-positive cells is dependent on MAPK^{ERK1,2} activation. Scale bar in panel A equals 25 μm, in panel B equals 100 μm, and in panel C equals 25 μm.